European Radiology (2019) 29:2034–2044
https://doi.org/10.1007/s00330-018-5734-2

MAGNETIC RESONANCE

Preoperative evaluation of small bowel complications in Crohn's disease: comparison of diffusion-weighted and contrast-enhanced MR imaging

M. Barat[1,2] · C. Hoeffel[3] · M. Bouquot[2,4] · A. S. Jannot[5,6] · R. Dautry[1] · M. Boudiaf[1] · K. Pautrat[4] · R. Kaci[7] · M. Camus[8] · C. Eveno[2,4,9] · M. Pocard[2,4,9] · P. Soyer[1,2,10] · A. Dohan[1,2,10]

Received: 14 March 2018 / Revised: 12 August 2018 / Accepted: 28 August 2018 / Published online: 9 October 2018

Abstract

Purpose To compare the accuracy of MR enterography (MRE) using combined T2-weighted and contrast-enhanced (CE) sequences with that of combined T2- and diffusion-weighted (DW) sequences for the detection of complex enteric Crohn's disease (CD).

Materials Thirty-eight patients who underwent surgery for CD complications and preoperative MRE from 2011 to 2016 were included. MRE examinations were blindly analyzed independently by one junior and one senior abdominal radiologist for the presence of fistula, stenosis and abscesses. During a first reading session, T2-weighted images (WI), steady-state sequences and DW-MRE were reviewed (set 1). During a separate distant session, T2-WI, True-FISP and CE-MRE were reviewed (set 2). Performance of each reader was evaluated by comparison with the standard of reference established using intraoperative and pathological findings.

Results Forty-eight fistulas, 43 stenoses and 11 abscesses were found. For the senior radiologist, sensitivity for the detection of fistula, stenosis and abscess ranged from 80% to 100% for set 1 and 88% to 100% for set 2 and specificity ranged from 56% to 70% for set 1 and 53% to 93% for set 2, with no significant difference between the sets (p = 0.342–0.429). For the junior radiologist, sensitivity ranged from 53% to 63% for set 1 and 64% to 88% for set 2 and specificity ranged from 0% to 25% for set 1 and 17% to 40% for set 2 (p = 0.001 and 0.007, respectively).

Conclusion For a senior radiologist, DW-MRE has similar sensitivity as CE-MRE for the detection of CD complications. For a junior radiologist, CE-MRE yields the best results compared with DW-MRE.

Key Points

- *For experienced readers, DWI has similar diagnostic capability as contrast-enhanced MR imaging for the diagnosis of Crohn's disease complications.*
- *For senior radiologists, gadolinium chelate injection could be waived for the diagnosis of Crohn's disease complications.*
- *The interpretation of DWI for Crohn's disease complications requires some experience.*

Keywords Crohn's disease · Magnetic resonance imaging · Comparative studies · Diffusion MRI

✉ M. Barat
maxime.barat89@gmail.com

[1] Department of Abdominal and Interventional Imaging, Hôpital Cochin, AP-HP, 27 rue du Faubourg St Jacques, 75014 Paris, France

[2] UMR INSERM 965, Hôpital Lariboisière, 2 rue Amboise Paré, 75010 Paris, France

[3] Department of Radiology, Hôpital Robert-Debré, Reims, France

[4] Department of Digestive and Oncologic Surgery, Hôpital Lariboisière, AP-HP, 2 rue Ambroise Paré, 75475 Paris cedex 10, France

[5] INSERM-UMRS 1138 Team 22, Cordeliers Research Center, Paris Descartes University, Paris, France

[6] Department of Medical Informatics and Public Health, European George Pompidou Hospital, AP-HP, 20 Rue Leblanc, 75015 Paris, France

[7] Department of Pathology, Hôpital Lariboisière, AP-HP, 2, rue Ambroise-Paré, 75010 Paris, France

[8] Department of Gastroenterology, Hôpital Saint-Antoine (AP-HP), Sorbonne University, Pierre et Marie Curie, Paris, France

[9] Université Sorbonne-Paris Cité, Paris-Diderot, 10 rue de Verdun, 75010 Paris, France

[10] Université Sorbonne Paris Cité, Paris-Descartes, 12 Rue de l'École de Médecine, 75006 Paris, France

Abbreviations

CD	Crohn's disease
CE	Contrast-enhanced
DWI	Diffusion-weighted imaging
HASTE	Half-Fourier acquisition single-shot turbo spin-echo
MRE	Magnetic resonance enterography
MRI	Magnetic resonance imaging
NA	Non applicable
NPV	Negative predictive value
PACS	Picture archiving and communication system
PPV	Positive predictive value
SD	Standard deviation
TNF	Tumor necrosis factor
TP	True positive
True-FISP	True fast imaging with steady-state precession
VIBE	Volumetric interpolated breath-hold examination
WI	Weighted imaging

Introduction

Crohn's disease (CD) is a chronic inflammatory disease of the gastrointestinal tract that can affect all segments [1]. Adults between 20 and 40 years old are mostly affected, and the total prevalence is about 10 for 100,000 persons per year [2]. The course of the disease is characterized by repetitive episodes of remission and recurrence. Chronic subclinical inflammation often leads to acute and chronic complications such as stricture, fistula or abscess and, after many years of evolution, cancer [3–5]. Treatment of CD consists of anti-inflammatory therapies using immunosuppressive drugs or anti-tumor necrosis factor (anti-TNF) agents [1]. Nonetheless, surgery is required for patients with clinically significant complications that do not respond to medical treatment. To avoid short bowel syndrome, surgery in CD patients should be as conservative and minimally invasive as possible. Therefore, optimal preoperative assessment of the lesions is paramount to select the best surgical approach [6–8].

Magnetic resonance enterography (MRE) is an effective modality for the preoperative assessment and monitoring of CD [8, 9]. Given the lack of radiation and high performance, MRE has become the standard of care in CD, especially in young patients [10]. The common protocol usually combines T2-weighted images (WI), fast dynamic steady-state sequences and T1-WI without and with intravenous administration of a gadolinium chelate. Contrast-enhanced (CE) T1-WI is the most informative sequence with a high degree of correlation with histopathological findings for wall thickness, inflammatory activity and detection of small bowel complications [11–14]. Several recent studies have evaluated diffusion-weighted imaging (DWI) in the assessment of CD activity and perianal fistula [15, 16]. Some authors have suggested that DWI could be equivalent or at least non-inferior to CE-T1-WI for the detection of CD inflammatory lesions [17–20]. Although many studies have suggested an added value for DWI in the diagnosis of CD complications, none has yet specifically compared its accuracy with that of other MR sequences [21, 22].

The safety of intravenous administration of a gadolinium chelate has become a matter of concern with nephrogenic systemic fibrosis and gadolinium deposition in the brain [23, 24]. These findings should lead physicians to use gadolinium chelates with caution. The purpose of this study was to compare the diagnostic accuracy of MRE using combined T2-weighted and contrast-enhanced (CE) sequences with that of combined T2- and diffusion-weighted (DW) sequences for the detection of complex enteric Crohn's disease (CD).

Materials and methods

Patients

This study was conducted following the recommendations of our institutional review board, and informed consent was obtained from all patients. We retrospectively searched the surgical database of our institution for all consecutive patients over 18 years old with CD who had surgery for small bowel complications of CD from January 2009 to December 2015. Patients who had no available preoperative CE-MRE and DWI examinations performed within 3 months before surgery were excluded. Fifty patients were originally identified in our surgical database. Of these, 12 patients were excluded because an MRE examination within the 3 preceding months was not available (3 patients), no resection had been performed during surgery or surgery was not performed for CD complication (9 patients). The study population ultimately consisted of 38 patients. There were 24 men and 14 women with a mean age of 31 ± 7 (SD) years (range: 18 - 50 years).

MRE protocol

All MRE examinations were performed with the same protocol, using a 1.5-T clinical MR unit (Magnetom Avanto®, VB15 software version, Siemens Healthineers) with 12 receiver channels, using 1 anterior torso phased-array coil with six channels and two posterior spine clusters with three channels each, with the patient in a supine position. The maximum gradient amplitude of the magnet was 45 mT/m with a maximal slew rate of 200 mT/m using quantum gradients. All patients drank 1.5 l of water containing polyethylene glycol at a dose of 64 g/l (Macrogol®, Biogaran) during the hour preceding the MRE examination. An intravenous injection of an antiperistaltic agent (glucagon 5.3 mg, GlucaGen®, Novo Nordisk Pharma) was performed during the examination before DWI and T1-contrast-enhanced sequences in all patients.

For all patients, the MRE protocol included breath-hold frequency-selective T2 half-Fourier acquisition single-shot turbo spin-echo (HASTE) sequences in the transverse and coronal planes, dynamic true fast imaging with steady-state precession (TrueFISP) in the transversal and coronal plane, and DWI and T1-weighted gradient echo fat-suppressed volumetric interpolated breath-hold examination (VIBE) weighted-imaging before and after multiphasic administration of gadolinium chelate (gadoterate meglumine, Dotarem®, Laboratoire Guerbet) in the transverse and coronal planes. Sequence parameters are shown in Table 1.

Images analysis

Two radiologists, one junior (senior resident with 3 years of experience in abdominal imaging and MRE, M. Ba.) and one senior (staff abdominal radiologist with more than 15 years of experience in abdominal imaging and MRE, M. Bo.) independently reviewed the anonymized MRE examinations on a picture-archiving and communication system (PACS) viewing station (DirectView®, 11.4.0.1253 sp1 version, Carestream Health Inc). Readings were performed during two separate sessions separated by a 3-month interval to avoid recall bias using a standardized form. Both readers analyzed HASTE, TrueFISP and DWI sequences (set 1) during the first session and the association of HASTE, TrueFISP and T1-weighted VIBE sequences obtained before and after intravenous administration of the gadolinium chelate during the second reading session (set 2).

For each set, the number of visible small bowel stenoses (i.e., small bowel lumen < 10 mm with or without prestenotic dilatation considering a prestenotic lumen > 30 mm for dilatation), their location and their length (in mm, measured using our viewing station system measuring tools by adding length of successive slices in the same plan), number of visible fistulas (abnormal communication between the small bowel and another organ) and their location (ileo-ileal, ileo-colic, ileo-sigmoid, sinus tract, entero-cutaneous, ileo-sacral, ileo-psoas), and the number of visible abscesses (encapsulated collection containing pus and/or gas) and their size were collected. For the two reading sessions, the study coordinator, who was aware of the standard of reference findings, was present and performed a lesion-to-lesion correlation [8].

Standard of reference

All included patients had surgery with peritoneal inspection and digestive resection. The standard of reference was established during a consensus review session among the study coordinator (AD), a senior radiologist, the senior abdominal pathologist who did all the pathological analyses (RK) and the senior surgeon who performed all the operations (KP). All patients had complete surgical exploration with a detailed surgical report. Gross examination of each pathological specimen was available with an extensive and detailed report. The study coordinator also had access to all imaging data and follow-up. For each patient, a list of visible lesions with their characteristics (i.e., size and location) on MRE was established as the standard of reference using a standardized data collection form. The pathologist reviewed the pathology

Table 1 MRI sequence parameters

Plane	T2-HASTE Transverse	T2-HASTE Coronal	TrueFISP Transverse	TrueFISP Coronal	T1-VIBE Transverse	DWI Transverse
TR/TE (ms/m^s)	1000/85	1000/85	3.9/1.95	3.53/1.77	385/3.07	4900/91
Field of view (mm)	350	380	400	460	400	380
Reconstruction matrix size	256 × 148	256 × 130	448 × 280	224 × 245	512 × 288	192 × 182
Voxel size (mm^3)	1.4 × 1.4 × 6.0	1.5 × 1.5 x 6.0	0.9 × 0.9 × 8.0	1.8 × 1.8 × 8.0	0.8 × 0.8 × 5.0	1.1 × 2.0 × 5.0
Intersection gap	30%	30%	50%	50%	0%	10%
Number of signal averages	1	1	2	2	1	4
Echo train length	256	256	1	1	1	NA
Echo spacing (ms)	8.4	8.4	12	12	12	0.83
Receiver bandwidth (Hz/pixel)	390	390	585	585	260	1302
Number of slices	35	20	30	20	32	35
Slices thickness (mm)	6	6	8	8	5	5
Turbo factor	23	23	16	16	4	NA
Grappa	NA	NA	NA	NA	NA	2
Acquisition time (s)	211	166	112	142	210	166
Diffusions directions	NA	NA	NA	NA	NA	3
b values (s/mm^2)	NA	NA	NA	NA	NA	0, 600, 1000

NA non-applicable

report, photographs of gross specimens and all available histopathological slices. The surgeon reviewed the surgical report and the intraoperative photographs when available. The lesions were assessed blinded to the reading in consensus and in an unblinded manner by the study coordinator (who was an independent senior radiologist), the senior surgeon and the senior pathologist who had all been implicated in the management of each of these patients.

Statistical analysis

Statistical analysis was performed using SPSS® statistics v22.0 (IBM Inc.). Descriptive statistics were calculated for all variables obtained with the three sequences and reported as mean, standard deviation (SD) and ranges for continuous variables and raw numbers, proportions and percentages for categorical variables. Sensitivity, specificity, positive predictive value (PPV), and negative predictive value (NPV) and accuracy for the detection of the different lesions were calculated for each MRI sequence. The McNemar test was used to search for differences in sensitivity between the different sequences. The Wilcoxon non-parametric paired signed test was used to compare quantitative variables. Inter-reader agreements for each lesion were calculated using the kappa test. Kappa coefficients between 0.00 and 0.20, 0.21 and 0.40, 0.41 and 0.60, 0.61 and 0.80, and 0.81 and 1.00 indicated slight, fair, moderate, substantial and almost perfect agreement, respectively [25]. Numbers of lesions found on each set by each reader were compared using the Student t-test. For all tests, a $p < 0.05$ was considered to indicate significance.

Results

Patient characteristics are summarized in Table 2. Among the 38 patients included, 31 had a total of 43 stenoses (mean length = 79 ± 48 [SD] mm; range: 10–280 mm), 28 patients had 43 fistulas (13 ileo-ileal, 12 ileo-cecal, 4 ileo-colic, 3 ileo-cutaneous, 3 ileo-sigmoid, 1 sinus tract, 1 ileo-sacral, 1 ileo-psoas and 1 recto-cutaneous) and 11 patients had 11 abscesses (mean size: 29 ± 9 [SD] mm; range: 10–50) (Table 2). The mean time between MRE examination and surgery was 36 ± 18 (SD) days (range: 2–90 days).

Considering set 1, inter-reader correlation was fair for the diagnosis of fistulas (kappa = 0.235) and for the diagnosis of stenosis (kappa = 0.066). For set 2, inter-reader correlation was moderate for the diagnosis of fistula (kappa = 0.512) and fair for the diagnosis of stenosis (kappa = 0.303). For the diagnosis of abscesses, inter-reader correlation was substantial for the both sets (set 1, kappa = 0.759; set 2, kappa = 0.679).

The sensitivity, specificity, PPV, NPV and accuracy for the diagnosis of CD complications for each set and each reader are summarized in Table 2. For the senior radiologist, using set 1, sensitivity and specificity for the diagnosis of fistula, stenosis and abscesses were not different from those with set 2 (respectively 80% versus 95%, 81% versus 88% and 100% versus 100% for sensitivity and 70% versus 53%, 56% versus 93% and 100% versus 100% for specificity [$p = 0.342$, $p = 0.384$ and $p = 0.429$ respectively]). Conversely, set 2 yielded significantly higher sensitivity and specificity for the diagnosis of all complications for the junior radiologist ($p < 0.001$, $p = 0.007$ and $p = 0.004$ respectively) (Figs. 1, 2, and 3).

When several lesions coexisted in the same patient, one was found by the junior radiologist compared with two lesions by the senior (mean number of lesions = 1 ± 0.6 for the junior radiologist versus 2 ± 0.7 lesions for the senior) ($p < 0.001$). Only small abscesses (i.e., < 30 mm in diameter) were missed by the junior radiologist (Table 3).

Table 2 Patient characteristics

Patients (*n*)	38
Age (years)[a]	31 ± 7.0 (18–50)
Gender (male/female)	24/ 14
Current smoker	5/38 (13%)
History of small bowel resection	15/38 (40%)
Time between diagnosis of CD and surgery (years)	6.8 ± 6.3 (0–15)
First onset of CD at the time of surgery	1/38 (2.5%)
Ongoing treatment	
No current treatment	14/38 (27%)
Immunotherapy	21/38 (55%)
Standard of reference	
Stenoses	43 in 31 patients
Length (mm)	97 ± 81 (10–350)
Fistulas	43 in 28 patients
	Ileo-colic: 4 Ileo-cecal: 12 Ileo-ileal: 13 Ileo-vesical: 4 Ileo-cutaneous: 3 Ileo-sigmoid: 3 Ileo-sacral: 1 sinus tract: 1 Ileo-psoas: 1 Recto-cutaneous: 1
Abscess	11 in 11 patients
Size (mm)	29 ± 9 (10–50)
Delay MRI – surgery (days)	36 ± 18 (2–90)
1–30 days (n)	17
31–60 days (n)	11
61–90 days (n)	10

Numbers in parentheses are percentages. Numbers in brackets are ranges

CD Chron's disease

[a] Mean ± SD

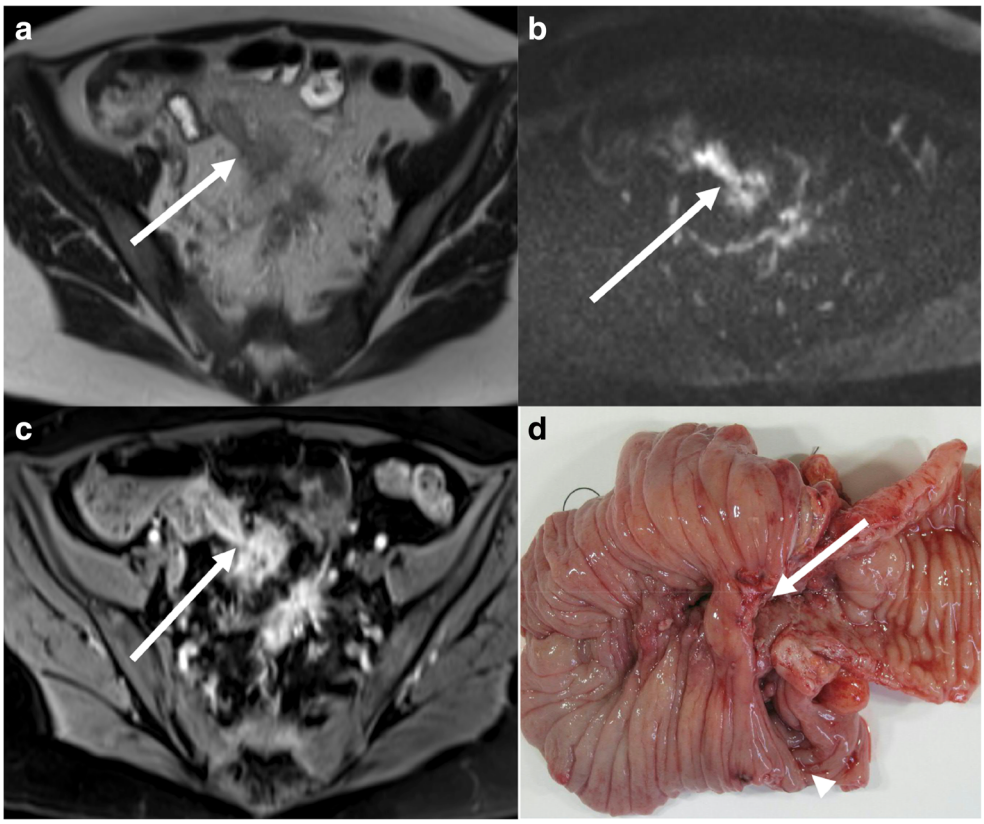

Fig. 1 A 33-year-old man with Crohn's disease treated with infliximab with pathologically proven ileo-colic fistulas. **a** T2 HASTE-weighted imaging in the transverse plane shows a linear fat infiltration from the ileum to the colon (arrow). **b** DW image in the transverse plane (b = 1000 s/mm^2) shows a linear zone of high restriction of the diffusion (arrow). **c** Contrast-enhanced T1 VIBE in the transverse plane shows a linear hyperintensity from the ileum to the colon (arrow). **d** Macroscopic view of the pathological analysis after ileo-cecal resection shows ileo-colic fistulas (arrow) next to the cecum (arrowhead)

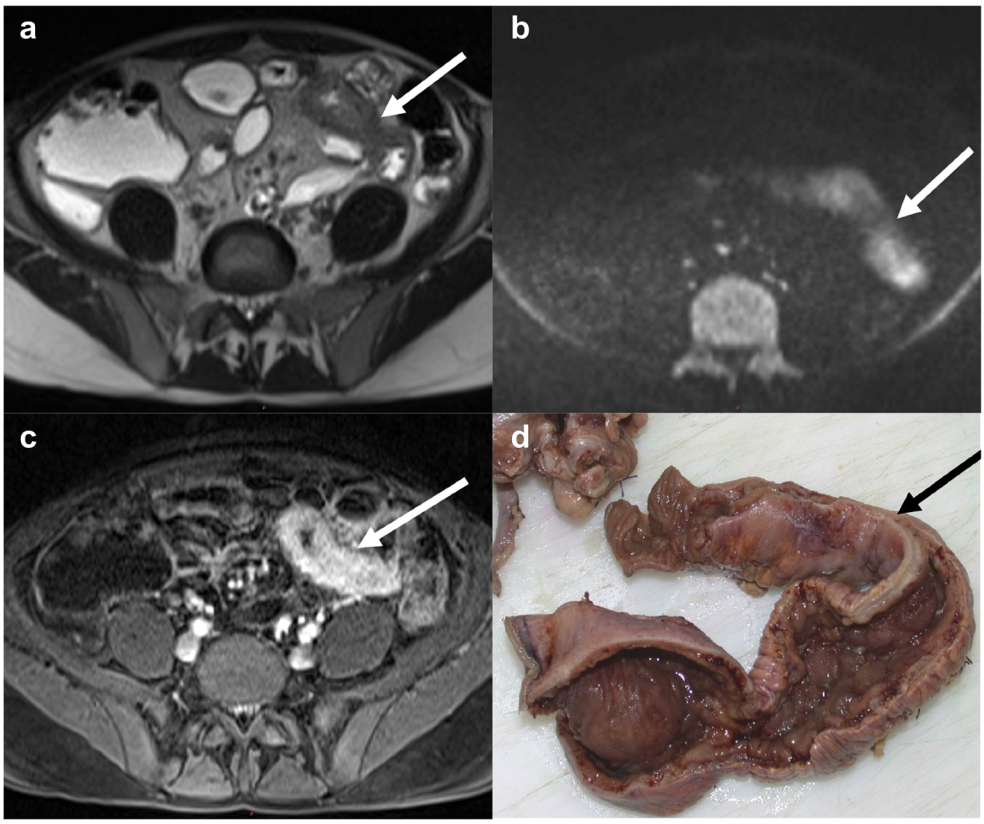

Fig. 2 A 29-year-old woman with Crohn's disease treated with oral steroids for 10 years with one jejunal and one ileal pathologically proven stenosis. **a** T2-HASTE-WI in the transverse plane shows a circumferential wall enlargement (arrow) with a reduction of the lumen size. **b** DW image in the transverse plane (b = 1000 s/mm^2) shows a restriction of the diffusion of the bowel wall that was thickened on the T2-HASTE-WI (arrow). **c** Contrast-enhanced-T1-VIBE in the transverse plane shows a circumferential wall enlargement with a hyper-enhancement (arrow) and a reduction of lumen size. **d** Macroscopic view of the pathological analysis after ileal resection shows an enlarged bowel wall and confirms the stenosis (arrow) with upstream bowel distension

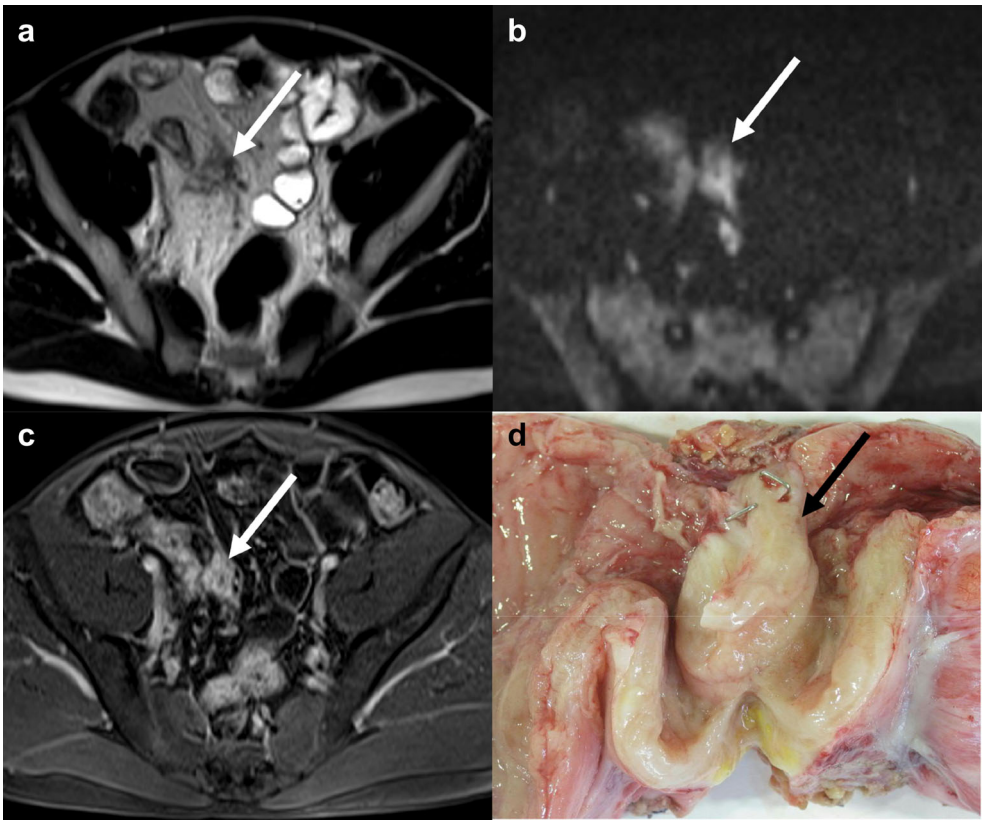

Fig. 3 A 33-year-old man with Crohn's disease, diagnosed 1 year ago, treated with oral corticoids, with a 25-mm mesenteric abscess, surgically and pathologically proven. **a** T2-HASTE-WI in the transverse plane shows a rounded infiltration of the pelvic fat, with blurred contours (arrow). **b** DW images in the transverse plane (b = 1000 s/mm^2) shows restricted diffusion in bowel wall in front of the fat stranding area that is optimally detected compared with A (arrow). **c** Contrast-enhanced T1 VIBE in the transverse plane shows a small rounded enhancing infiltration of the fat with a discrete central hyposignal (arrow). **d** Photograph shows gross specimen after surgery. A 25-mm mesenteric abscess (arrow) is histopathologically confirmed

Length of stenoses was always overestimated compared with the standard of reference except by the senior radiologist using set 1 (97 ± 81 [SD] mm; range: 10–350 mm versus 95 ± 69 [SD] mm; range: 10–250 mm [$p = 0.92$]). Sizes of abscesses on MRE were similar to sizes as established using the standard of reference for the two readers and for the two sets ($p = 0.210$–0.644) (Table 4).

Considering the 43 stenoses, the junior reader missed 13 lesions with set 1 and 4 using set 2, while the senior radiologist missed 4 lesions using set 1 and 1 stenosis using set 2 (Table 3). The junior reader missed the shortest stenoses: 44 ± 23 (SD) mm for undepicted stenoses versus 140 ± 86 (SD) mm for depicted stenoses using set 1 ($p < 0.001$). The missed stenoses were also shorter using set 2 (22 ± 16 [SD] mm versus 110 ± 81 [SD] mm, $p = 0.022$). For the senior reader, no differences in terms of length were found between depicted and undepicted stenoses ($p = 0.173$ and 0.587 for set 1 and set 2, respectively). All stenoses shorter than 30 mm were missed by the junior radiologist with both sets, and all stenoses longer than 100 mm were depicted by both readers using either imaging set.

Considering the 43 fistulas in 28 patients, the FN rates were especially high for ileo-sigmoid fistula with set 1 for the junior radiologist (4/4 fistulas missed) while only 1/4 fistula was missed with set 2 (Table 5). Less common complex fistula locations (i.e., ileo-vesical [$n = 1$], recto-cutaneous [$n = 1$] and ileo-psoas [$n = 1$] fistulas) were all depicted by the two radiologists with both sets. Considering abscesses, the junior reader did not depict abscesses < 30 mm in size (5 abscess missed with both sets). The senior reader missed one abscess using set 1 but none using set 2.

Discussion

Our study suggests that MRE performed with the association of T2-WI and DWI sequences without intravenous gadolinium chelate is an alternative to the more classical protocol including CE-T1-WI without DWI for the diagnosis of stenosis, fistula and abscess complicating CD, which is in line with previous studies [18, 26, 27]. Sensitivity and specificity of set 1 and set 2 were not different for the senior radiologist. However, our study shows that the reading of DWI requires more experience than CE-T1-WI, as the junior radiologist obtained significantly lower sensitivity and specificity with set 1 compared with set 2.

Increasing evidence is now available to suggest that DWI is accurate in CD but, for Europeans societies, the use of DWI remains optional [18, 21, 22, 28]. However, the low performance of the junior radiologist obtained with set 1 in our study suggests that CE sequences may still be needed to facilitate reading, especially for inexperienced readers [20, 29].

Using high b values, DWI shows hyperintense, linear, retractile images suggestive of internal fistulas, sometimes attracting structures or associated with an inflammatory mass [17]. In a series including 14 patients, Schmid-Tannwald et al found a similar detection rate of internal fistulas using T2-WI

Table 3 Sensitivity, specificity, PPV, NPV, accuracy and kappa values for the detection of acute CD complications for each set of reading, for each reader using the combination of surgical and pathological findings as gold standard

		SR	TP	TN	FP	FN	Sensitivity	Specificity	PPV	NPV	Accuracy	*p* value[a]	Kappa value between set 1 and set 2 for each reader[b]	Kappa value between reader 1 and reader 2 for each reading set[b]
Reader 1 (senior)	***Set 1***													
	Fistula	**43**	36	7	9	3	0.80 (0.67-0.89)	0.70 (0.40-0.90)	0.92 (0.80-0.97)	0.42 (0.31-0.54)	0.78 (0.70-0.89)			
	Stenosis	**43**	31	5	7	4	0.81 (0.67-0.91)	0.56 (0.27-0.81)	0.88 (0.74-0.94)	0.41 (0.27-0.57)	0.77 (0.68-0.89)			
	Abscess	**11**	10	0	0	1	1.00 (0.74-1.00)	NA	0.91 (0.69-0.99)	NA	0.91 (0.79-100)			
	Set 2													
	Fistula	**43**	40	8	9	2	0.95 (0.84-0.99)	0.53 (0.31-0.79)	0.82 (0.71-0.92)	0.80 (0.55-1.00)	0.81 (0.74-0.91)	0.342	0.512	
	Stenosis	**43**	35	13	5	1	0.88 (0.74-0.95)	0.93 (0.69-0.98)	0.88 (0.0-1.00)	0.93 (0.79-1.00)	0.89 (0.83-0.97)	0.384	0.303	
	Abscess	**11**	11	0	0	0	1.00 (0.74-1.00)	NA	NA	NA	1.00	0.429	0.679	
Reader 2 (junior)	***Set 1***													
	Fistula	**43**	16	0	12	14	0.53 (0.32-0.70)	0.00 (0.00-0.24)	0.57 (0.38-0.68)	NA	0.39 (0.27-0.53)			0.235
	Stenosis	**43**	22	2	6	13	0.63 (0.46-0.77)	0.25 (0.07-0.59)	0.78 (0.63-0.94)	0.13 (0.00-0.31)	0.56 (0.44-0.71)			0.066
	Abscess	**11**	6	0	0	5	0.55 (0.28-0.79)	NA	NA	NA	0.55 (0.31-0.84)			0.679
	Set 2													
	Fistula	**43**	29	2	10	5	0.86 (0.70-0.94)	0.17 (0.05-0.45)	0.74 (0.61-0.88)	0.28 (0.00-0.62)	0.67 (0.57-0.81)	**< 0.001**	0.552	0.527
	Stenosis	**43**	29	4	6	4	0.88 (0.73-0.95)	0.40 (0.17-0.69)	0.83 (0.70-0.95)	0.50 (0.15-0.85)	0.77 (0.68-0.89)	**0.007**	0.37	0.303
	Abscess	**11**	7	0	0	4	0.64 (0.35-0.85)	NA	NA	NA	0.64 (0.41-0.92)	**0.004**	0.732	0.759

Set 1 means the association of DWI and T2-weighted imaging. Set 2 means T1-FS-weighted imaging with and without injection of gadolinium chelate. Numbers in bold indicate significant *p* value

SR standard of reference, *TP* true positive, *TN* true negative, *FP* false positive, *FN* false negative, *PPV* positive predictive value, *NPV* negative positive value, *NA* non-applicable

[a] McNemar test for sensitivity.

[b] Cohen kappa correlation test

Table 4 Comparison of stenosis length and abscess size for the two sets of different readers with the standard of reference

		Mean ± SD (range)	p^a	p^b
Stenosis length	Standard of reference	97 ± 81 (10–350)		
	Senior set 1	95 ± 69 (10–250)	0.922	
	Senior set 2	167 ± 117 (40–600)	**0.007**	
	Junior set 1	179 ± 107 (20–550)	**0.001**	0.628
	Junior set 2	171 ± 117 (40–600)	< **0.001**	0.349
Abscess size	Standard of reference	29 ± 9 (10–50)		
	Senior set 1	33 ± 15 (16–70)	0.644	
	Senior set 2	31 ± 15 (13–65)	0.609	
	Junior set 1	34 ± 14 (17–65)	0.345	0.671
	Junior set 2	38 ± 20 (13–70)	0.210	0.272

Numbers in bold indicate significant difference

[a] Student *t*-test comparing measures with the standard of reference

[b] Student *t*-test comparing measures of each set between reader 1 and reader 2

and DWI (set 1) than using T2-WI and CE-T1-WI sequences (set 2) [21]. Even though the role of DWI for the diagnosis of perianal complications such as fistula is now well accepted, no other study has specifically evaluated the role of DWI for the diagnosis of internal fistula in CD patients [22, 30, 31]. Considering bowel stenosis, CE-T1-WI has proven efficacy for the depiction of stenosis and is helpful to differentiate acute from chronic lesions according to the pattern of bowel wall enhancement [32]. Similarly, DWI has demonstrated utility for the evaluation of CD activity with a high degree of correlation with histopathological findings but its usefulness for diagnosing stenosis has not yet been studied [33]. Finally, for the diagnosis of extra-luminal CD complications, including fistula and abdominal or pelvic abscesses, DWI has a sensitivity that reaches up to 90% with a very high specificity but has not been evaluated for this specific condition of CD complications in the preoperative diagnosis setting [18, 34].

For the junior radiologist, diagnostic performances with set 1 were lower than those of the senior radiologist. We assume that reading of DWI, which provides thicker slices than T1-weighted VIBE sequences (5 vs. 1.2 mm, respectively), and the loss of anatomical and morphological details on high b value DW images require a more important learning curve, although this hypothesis has not been fully elucidated so far [26, 27]. When analyzing the readings of the junior radiologist, we observed that only one lesion was detected with DWI in patients with multiple coexisting lesions. Concerning abscesses, only the smaller ones (i.e., < 30 mm) were missed by reader 2. The same result was found for stenoses as only long stenoses were detected by the junior radiologist. Considering fistulas, the most frequently missed lesions were loco-regional fistulas, between two bowel segments, which are also the most frequent lesions. These findings suggest that a learning curve for DWI sequence analysis as well as a good knowledge of the disease and of the high prevalence of co-existing lesions is required.

Several kinds of information can be obtained using different models of analysis of DW-MRI. The diffusion measurement using a mono-exponential model requires a few numbers of b values and has a proven diagnostic value for lesion characterization [35–37]. When many b values are used, bi- or tri-

Table 5 Sensitivity for the detection of fistulas for the different sets considering their location

	Standard of reference	Junior set 1	Junior set 2	Senior set 1	Senior set 2
Ileo-colic	4	25%	25%	75%	75%
Ileo-sigmoid	4	0%	75%	100%	100%
Ileo-cecal	12	50%	50%	50%	83%
Ileo-ileal	12	25%	67%	83%	92%
Ileum-bladder	4	100%	100%	100%	100%
Ileo-cutaneous	3	67%	100%	100%	100%
Ileo-sacral	1	0%	100%	100%	100%
Sinus tract	1	0%	100%	100%	100%
Ileo-psoas	1	100%	100%	100%	100%
Recto-cutaneous	1	100%	100%	100%	100%

Set 1: association of DWI, TrueFISP and T2-WI

Set 2: association of T1-FS with and without injection of gadolinium chelate, TrueFISP and T2-WI

exponential models can be used and the perfusion fraction, pseudo-diffusion fraction or kurtosis can be calculated, thus providing functional information in many diseases [38–40]. In our study and for CD in general, a mono-exponential model was used for DWI in MRE [17]. Histopathological changes in CD mostly consist of high-density lymphatic cell infiltration, epithelioid granuloma and edema [41]. Even though HASTE provides direct and indirect signs for the diagnosis of CD complications, as in many other abdominal diseases, DWI sequences may facilitate the detection of these lesions [42]. Moreover, smaller abscesses may be missed on unenhanced MR images. DWI, ensuring a high tissue contrast, may increase abscess detection, which is paramount, particularly before using immunosuppressive drugs [43].

The major strength of our study compared with other pre-existing studies is to focus on all surgical complications with a pathological and surgical correlation [21]. Moreover, we used a double-blinded reading, allowing evaluation of inter-reader correlations and the impact of radiologist experience. Nonetheless, our study has several limitations including a monocentric setting, a retrospective design and the rather small number of patients, thus potentially inducing a recruitment bias. As MRE plays a pivotal role in the management of these patients and in making the decision for surgery, some patients may have been excluded as they did not have surgery because of missed significant lesions on MRE. Some patients may also have been excluded because MRE was not performed with the 3 preceding months. As CE-T1-WI sequences are currently the gold standard, this study is actually a non-inferiority study comparing a less invasive diagnosis test (DWI) with the standard one. Using the formula for sample size for a non-inferiority study comparing diagnostic tests based on paired observations [44], assuming a power of 80%, a type-one error of 5% and a prevalence of 0.7, we estimated that 45 samples would be required to show that set 1 is non-inferior to set 2 if we chose a 20% difference in sensitivity and a 20% difference in specificity as our minimum acceptable differences. As these differences are larger than what is currently assumed for a non-inferiority study, our study is somehow underpowered: the small significant difference in sensitivity and specificity could be highlighted with a larger sample size. Another limitation may relate to recall bias because some complex CD patient images are often very memorable and, because of the reading in two sets, readers can memorize findings on the first imaging set. We tried to limit this bias with different tools: anonymization, reading of sets in a random manner and an interval of 3 months between the two reading sets. As the reading session for set 1 preceded the reading sessions for set 2 in all patients, we assume that the performance of set 2 may have been overestimated because of recall bias. However, as CE-T1-WI is the standard reference sequence, and because we did not expect set 1 to surpass set 2, we preferred to avoid the recall bias for the reading of set 1, which was the set we were assessing.

Then, the retrospective design did not allow evaluating the inflammatory mass often associated with fistulae, but not usually reported by pathologists, and extra-intestinal abdominal complications [17]. However, our promising results constitute a first step to further prospective multicentric and controlled studies. Finally, due to the small number of fistulas for each location, we were not able to perform a reliable statistical analysis for the location diagnosis accuracy.

In conclusion, for an experienced abdominal radiologist, DWI may replace CE-T1-WI for the preoperative diagnosis of CD complications with MRE. We suggest that for the specific case of suspicion of CD complications, a simple protocol using morphological T2-weighted MR images associated with DWI could be efficacious in first intention. The intravenous administration of a gadolinium-based contrast agent should be considered in second intention in specific situations. These results need to be confirmed with larger and prospective studies and could favor decreasing use of gadolinium chelate injection in CD patients.

Funding The authors state that this work has not received any funding.

Compliance with ethical standards

Guarantor The scientific guarantor of this publication is P. Soyer, MD, PhD.

Conflict of interest The authors of this manuscript declare no relationships with any companies, whose products or services may be related to the subject matter of the article.

Statistics and Biometry Statistical analysis was performed by an expert senior statistician (Dr. AS Jannot)

Informed Consent Written informed consent was obtained from all subjects (patients) in this study.

Ethical Approval Institutional Review Board approval was obtained.

Methodology
- retrospective
- diagnosis method
- performed at one institution

References

1. Torres J, Mehandru S, Colombel JF, Peyrin-Biroulet L (2017) Crohn's disease. Lancet 389:1741–1755
2. Molodecky NA, Soon IS, Rabi DM et al (2012) Increasing incidence and prevalence of the inflammatory bowel diseases with time, based on systematic review. Gastroenterology 142:46–54 e42 quiz e30

3. Pariente B, Cosnes J, Danese S et al (2011) Development of the Crohn's disease digestive damage score, the Lemann score. Inflamm Bowel Dis 17:1415–1422
4. Barral M, Dohan A, Allez M et al (2016) Gastrointestinal cancers in inflammatory bowel disease: an update with emphasis on imaging findings. Crit Rev Oncol Hematol 97:30–46
5. Hristova L, Soyer P, Hoeffel C et al (2013) Colorectal cancer in inflammatory bowel diseases: CT features with pathological correlation. Abdom Imaging 38:421–435
6. Goyer P, Alves A, Bretagnol F, Bouhnik Y, Valleur P, Panis Y (2009) Impact of complex Crohn's disease on the outcome of laparoscopic ileocecal resection: a comparative clinical study in 124 patients. Dis Colon Rectum 52:205–210
7. Harb WJ (2015) Crohn's Disease of the Colon, Rectum, and Anus. Surg Clin North Am 95(1195-1210):vi
8. Malgras B, Soyer P, Boudiaf M et al (2012) Accuracy of imaging for predicting operative approach in Crohn's disease. Br J Surg 99: 1011–1020
9. Stoddard PB, Ghazi LJ, Wong-You-Cheong J, Cross RK, Vandermeer FQ (2015) Magnetic resonance enterography: state of the art. Inflamm Bowel Dis 21:229–239
10. Van Assche G, Dignass A, Panes J et al (2010) The second European evidence-based Consensus on the diagnosis and management of Crohn's disease: Definitions and diagnosis. J Crohns Colitis 4:7–27
11. Zappa M, Stefanescu C, Cazals-Hatem D et al (2011) Which magnetic resonance imaging findings accurately evaluate inflammation in small bowel Crohn's disease? A retrospective comparison with surgical pathologic analysis. Inflamm Bowel Dis 17:984–993
12. Pola S, Santillan C, Levesque BG, Feagan BG, Sandborn WJ (2014) An overview of magnetic resonance enterography for Crohn's disease. Dig Dis Sci 59:2040–2049
13. Erden A, Ünal S, Akkaya HE et al (2017) MR Enterography in Crohn's disease complicated with enteroenteric fistula. Eur J Radiol. https://doi.org/10.1016/j.ejrad.2017.06.012
14. You-Ling Shyu J, Chick JF, Adackapara CA, Adduci AJ (2016) Urachal-colonic fistula: MR imaging and MDCT features. Diagn Interv Imaging 97:105–108
15. Dohan A, Eveno C, Oprea R et al (2014) Diffusion-weighted MR imaging for the diagnosis of abscess complicating fistula-in-ano: preliminary experience. Eur Radiol 24:2906–2915
16. Monnier L, Dohan A, Amara N et al (2017) Anoperineal disease in hidradenitis suppurativa: MR imaging distinction from perianal Crohn's disease. Eur Radiol 27:4100–4109
17. Dohan A, Taylor S, Hoeffel C et al (2016) Diffusion-weighted MRI in Crohn's disease: Current status and recommendations. J Magn Reson Imaging 44:1381–1396
18. Seo N, Park SH, Kim KJ et al (2016) MR enterography for the evaluation of small-bowel inflammation in Crohn disease by using diffusion-weighted imaging without intravenous contrast material: a prospective noninferiority study. Radiology 278: 762–772
19. Sinha R, Rajiah P, Ramachandran I, Sanders S, Murphy PD (2013) Diffusion-weighted MR imaging of the gastrointestinal tract: technique, indications, and imaging findings. Radiographics 33:655–676
20. Tielbeek JA, Ziech ML, Li Z et al (2014) Evaluation of conventional, dynamic contrast enhanced and diffusion weighted MRI for quantitative Crohn's disease assessment with histopathology of surgical specimens. Eur Radiol 24:619–629
21. Schmid-Tannwald C, Agrawal G, Dahi F, Sethi I, Oto A (2012) Diffusion-weighted MRI: role in detecting abdominopelvic internal fistulas and sinus tracts. J Magn Reson Imaging 35:125–131
22. Cavusoglu M, Duran S, Sozmen Ciliz D et al (2017) Added value of diffusion-weighted magnetic resonance imaging for the diagnosis of perianal fistula. Diagn Interv Imaging 98:401–408
23. Olchowy C, Cebulski K, Łasecki M et al (2017) The presence of the gadolinium-based contrast agent depositions in the brain and symptoms of gadolinium neurotoxicity - A systematic review. PLoS One 12:e0171704
24. Soyer P, Dohan A, Patkar D, Gottschalk A (2017) Observational study on the safety profile of gadoterate meglumine in 35,499 patients: The SECURE study. J Magn Reson Imaging 45:988–997
25. Landis JR, Koch GG (1977) The measurement of observer agreement for categorical data. Biometrics 33:159–174
26. Seastedt KP, Trencheva K, Michelassi F et al (2014) Accuracy of CT enterography and magnetic resonance enterography imaging to detect lesions preoperatively in patients undergoing surgery for Crohn's disease. Dis Colon Rectum 57:1364–1370
27. Schmidt S, Chevallier P, Bessoud B et al (2007) Diagnostic performance of MRI for detection of intestinal fistulas in patients with complicated inflammatory bowel conditions. Eur Radiol 17:2957–2963
28. Taylor SA, Avni F, Cronin CG et al (2017) The first joint ESGAR/ESPR consensus statement on the technical performance of cross-sectional small bowel and colonic imaging. Eur Radiol 27:2570–2582
29. Fiorino G, Bonifacio C, Peyrin-Biroulet L et al (2011) Prospective comparison of computed tomography enterography and magnetic resonance enterography for assessment of disease activity and complications in ileocolonic Crohn's disease. Inflamm Bowel Dis 17: 1073–1080
30. Baik J, Kim SH, Lee Y, Yoon JH (2017) Comparison of T2-weighted imaging, diffusion-weighted imaging and contrast-enhanced T1-weighted MR imaging for evaluating perianal fistulas. Clin Imaging 44:16–21
31. Yoshizako T, Wada A, Takahara T et al (2012) Diffusion-weighted MRI for evaluating perianal fistula activity: feasibility study. Eur J Radiol 81:2049–2053
32. Rimola J, Planell N, Rodríguez S et al (2015) Characterization of inflammation and fibrosis in Crohn's disease lesions by magnetic resonance imaging. Am J Gastroenterol 110:432–440
33. Li XH, Sun CH, Mao R et al (2017) Diffusion-weighted MRI enables to accurately grade inflammatory activity in patients of ileocolonic Crohn's disease: results from an observational study. Inflamm Bowel Dis 23:244–253
34. Nguyen TL, Soyer P, Barbe C et al (2013) Diagnostic value of diffusion-weighted magnetic resonance imaging in pelvic abscesses. J Comput Assist Tomogr 37:971–979
35. Norris DG, Niendorf T, Leibfritz D (1994) Health and infarcted brain tissues studied at short diffusion times: the origins of apparent restriction and the reduction in apparent diffusion coefficient. NMR Biomed 7:304–310
36. Sugahara T, Korogi Y, Kochi M et al (1999) Usefulness of diffusion-weighted MRI with echo-planar technique in the evaluation of cellularity in gliomas. J Magn Reson Imaging 9:53–60
37. Chan JH, Tsui EY, Luk SH et al (2001) Diffusion-weighted MR imaging of the liver: distinguishing hepatic abscess from cystic or necrotic tumor. Abdom Imaging 26:161–165
38. Le Bihan D, Breton E, Lallemand D, Aubin ML, Vignaud J, Laval-Jeantet M (1988) Separation of diffusion and perfusion in intravoxel incoherent motion MR imaging. Radiology 168: 497–505
39. Le Bihan D, Breton E, Lallemand D, Grenier P, Cabanis E, Laval-Jeantet M (1986) MR imaging of intravoxel incoherent motions:

application to diffusion and perfusion in neurologic disorders. Radiology 161:401–407
40. Rosenkrantz AB, Padhani AR, Chenevert TL et al (2015) Body diffusion kurtosis imaging: Basic principles, applications, and considerations for clinical practice. J Magn Reson Imaging 42:1190–1202
41. Yantiss RK, Odze RD (2006) Diagnostic difficulties in inflammatory bowel disease pathology. Histopathology 48:116–132
42. Nasu K, Kuroki Y, Nawano S et al (2006) Hepatic metastases: diffusion-weighted sensitivity-encoding versus SPIO-enhanced MR imaging. Radiology 239:122–130
43. Oto A, Schmid-Tannwald C, Agrawal G et al (2011) Diffusion-weighted MR imaging of abdominopelvic abscesses. Emerg Radiol 18:515–524
44. Lu Y, Jin H, Genant HK (2003) On the non-inferiority of a diagnostic test based on paired observations. Stat Med 22:3029–3044